Dalton Transactions

RSC Publishing

PAPER

View Article Online
View Journal | View Issue

Cite this: *Dalton Trans.*, 2013, **42**, 8394

Reversible multicomponent self-assembly mediated by bismuth ions†

Amber M. Johnson, Michael C. Young and Richard J. Hooley*

Received 1st March 2013,
Accepted 14th April 2013

DOI: 10.1039/c3dt50578b

www.rsc.org/dalton

Bi(III) ions are capable of reversible, multicomponent self assembly with suitable tris-coordinate ligands. The nature of the self-assembled structures observed are dependent on the ligand coordination geometry, ligand protonation state and Bi concentration. These assemblies can exploit the maximum number of coordination sites at the Bi vertices (nine), and the self-assembly process has been studied by 1D NMR, Diffusion NMR, ESI-MS and X-ray crystallographic analysis. V-shaped coordinating ligands reversibly form discrete M_2L_4, M_2L_3, and M_2L_2 complexes dependent on ligand/bismuth concentration, whereas a linear coordinating ligand forms a single discrete M_3L_3 assembly.

Introduction

The self-assembly of organic ligands with metals is a powerful tool for the synthesis of complex three-dimensional structures.[1] These assemblies offer advantages over covalent macromolecules in that they are held together by weaker bonds, allowing mismatches to break apart and reassemble into the most thermodynamically stable structures.[2] Typically transition metals, with their well-defined coordination spheres and numerous characterized Werner complexes, are utilized for this purpose. By matching ligands and metals with complementary geometric constraints, many of these self-assembled polygons[3] and polyhedra[4] have been synthesized. Polyhedral cages targeted in this method have shown uses ranging from selective guest binding[5] to novel stereo and regioselectivity[6] not commonly observed with traditional catalysts. Transition metal complexes can be challenging to study, however: transition metals often display paramagnetism and can easily access varying oxidation states, leading to air and water sensitivity of solution-phase cage complexes and complex (or inaccessible) NMR spectra. As the size and complexity of the assemblies increases, the formation of a single discrete product can become challenging or even impossible.[7] The use of main group metals as vertices for metal-mediated self-assembly would solve these challenges by providing air and water stable diamagnetic assemblies with a single consistent oxidation state.

Examples of self-assembled structures controlled by main group metals are quite uncommon, however. Group 13 metals such as aluminum and gallium have been shown to make self-assembled cages analogous to those of transition metals, but are limited by their high charge : size ratio to hard, oxygen-containing ligands.[8] Larger main group metals can display a large range of coordination geometries and often lack the predictable angles associated with transition metals that allow for predictable multicomponent self-assembly. A limited number of self-assembled structures of other main-group metals are known,[9] including those of arsenic,[9a–d] germanium,[9e] tin,[9f,g] lead,[9h,i] and antimony[9j,k]. A metal that has received relatively little attention in this field is the largest stable metal, bismuth. Recent interest in the coordination chemistry of bismuth has primarily focused on its potential medical applications.[10]

The coordination sphere of bismuth, however, offers far more variety than that of smaller main-group metals.[11] With multiple possibilities in coordination number, the use of bismuth as a structural component in supramolecular self-assembly could allow for controlled switchable self-assemblies using a single metal type, something that can be difficult for transition metals with more rigidly defined coordination geometry. The larger coordination sphere of bismuth(III) at first seems reminiscent of the lanthanides, but nine-coordinate Bi(III) species are rare, and have never been observed to mediate the self-assembly of metal–organic cages.[12] This is in contrast to lanthanides, which in their +3 state can easily form 9-coordinate complexes.[13]

Bismuth ions have, to date, only been exploited for supramolecular assembly in their tri-coordinate state, as an analog of As and Sb-controlled assembly involving bis-thiolate ligands as single-point coordinators for two bismuth(III) ions.[14]

Department of Chemistry, University of California – Riverside, 501 Big Springs Rd, Riverside, CA 92521, USA. E-mail: richard.hooley@ucr.edu; Fax: +1 951-827-4713; Tel: +1 951-827-4924

†Electronic supplementary information (ESI) available: Synthetic procedures and selected NMR, mass spectral, and X-ray diffraction data. CCDC 892045. For ESI and crystallographic data in CIF or other electronic format see DOI: 10.1039/c3dt50578b

To access larger structures with predictable self-assembly properties, the full coordination sphere of Bi(III) must be exploited. The simplest strategy is to apply tridentate chelator ligands, three of which can assemble around each Bi ion. Recent work with lanthanide-mediated self-assembly has shown that hydrazones derived from 2-pyridine carboxaldehyde and salicylaldehyde can be effective chelators for these non-transition metals with larger coordination spheres.[15] Here we exploit the variable coordination sphere of bismuth to access reversible multicomponent self-assemblies upon addition of suitable tridentate chelating ligands.

Results and discussion

Two ligands (**1** and **2**) were used to study the self-assembly properties of Bi(III) ions, providing different coordination angles for self-assembly. V-shaped ligand **1** was synthesized in three steps as shown in Fig. 1. Double Suzuki coupling between 1,3-dibromobenzene and 4-ethoxycarbonylphenylboronic acid gave the corresponding terphenyl diester in 64% yield, which was converted to the corresponding hydrazide **3** in 86% yield by refluxing in anhydrous hydrazine. The desired metal-coordinating hydrazone species **1** was formed by the combination of **3** and commercially available 2-formylpyridine under acidic conditions. The linear equivalent **2** was accessed from commercially available biphenyl-4,4′-dicarboxylic acid. In this case, formation of hydrazide **4**[16] was achieved directly from the diacid through HCTU coupling with anhydrous hydrazine in 76% yield. The bis-hydrazide was then treated with 2-formylpyridine as before to give bis-hydrazone **2**.

Initial self-assembly tests were analyzed by ^{1}H NMR spectroscopy. Hydrazone ligand **1** is only sparingly soluble in acetonitrile, but is rapidly solubilized by addition of substoichiometric amounts of bismuth(III) triflate. Upon titration of $Bi(OTf)_3$ into a CD_3CN solution/suspension of **1**, downfield shifts were observed in the ^{1}H NMR spectrum (see Fig. 2 and ESI†), consistent with metal–ligand coordination. After addition of 0.50 mol eq. $Bi(OTf)_3$, only one species was observed in the ^{1}H NMR spectrum. The simplest analysis of the coordination can be performed by studying *ortho*-pyridyl proton H_1 and imine proton H_2 upon complexation, observed

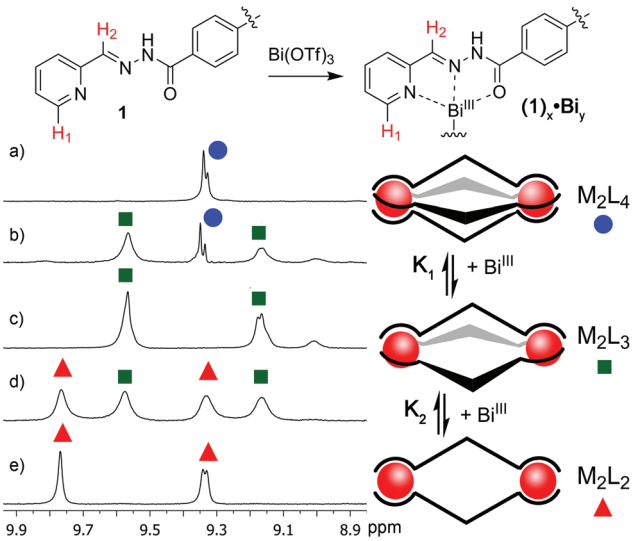

Fig. 2 ^{1}H NMR titration of $Bi(OTf)_3$ into ligand **1** (400 MHz, 298 K, CD_3CN): (a) 0.5 eq.; (b) 0.67 eq.; (c) 1 eq.; (d) 2 eq.; (e) 3 eq.

in the downfield region of the spectrum (Fig. 2, for full spectra, see ESI†). Upon further addition of $Bi(OTf)_3$, peaks for a second species grow in with concomitant decrease in intensity for the original complex (Fig. 2b). After addition of 2 mol eq. $Bi(OTf)_3$, a third species is observed (Fig. 2d), and this species becomes dominant after addition of 3 mol eq. $Bi(OTf)_3$. This shows the versatility of bismuth compared to transition metals, which do not show this variable coordination.[17]

The NMR titration data suggested that the three observed complexes displayed M_2L_2, M_2L_3 and M_2L_4 stoichiometries, shown in cartoon form in Fig. 2. All NH protons are retained in the NMR spectra of the assemblies, suggesting that the complex formation occurs with neutral ligand, leading to positively charged assemblies. The mixtures were also subjected to ESI-MS analysis to corroborate this assignment. A sample of M_2L_2 complex was prepared by combining ligand and $Bi(OTf)_3$ in acetonitrile. After confirmation of the presence of a single M_2L_2 complex in solution by ^{1}H NMR analysis, the solution was ionized under mild electrospray conditions. Upon ionization, all three components were observed in the mass spectrum, as shown in Fig. 3. Each complex (**1_2·Bi$_2$**, **1_3·Bi$_2$**, and

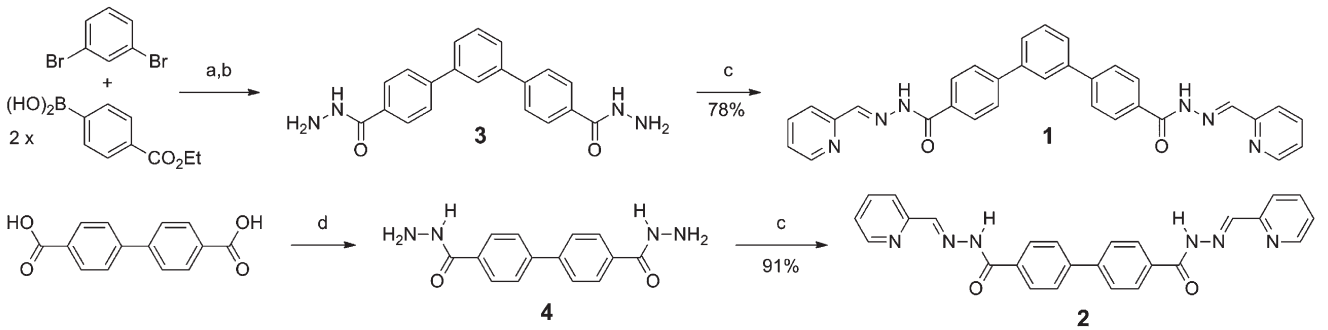

Fig. 1 Synthesis of ligands **1** and **2**. (a) 5% $PdCl_2(PPh_3)_2$, Cs_2CO_3, DMF, 100 °C, 64%; (b) N_2H_4, 85 °C, 86%; (c) 2-formylpyridine, 5% AcOH, EtOH, reflux; (d) HCTU, Et_3N, N_2H_4, 76%.

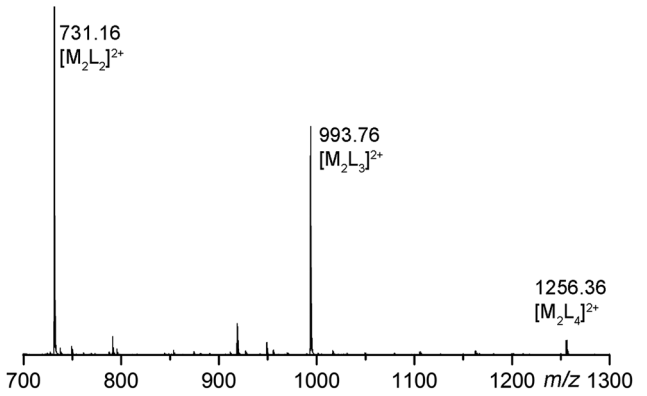

Fig. 3 ESI-MS spectrum of **1** + $Bi(OTf)_3$, indicating formation of the $\mathbf{1_2{\cdot}Bi_2}$, $\mathbf{1_3{\cdot}Bi_2}$ and $\mathbf{1_4{\cdot}Bi_2}$ complexes.

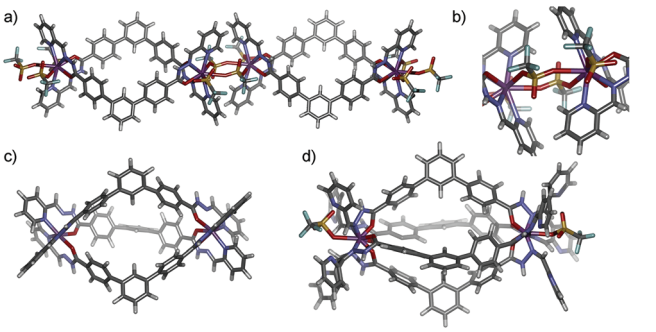

Fig. 4 (a) X-Ray diffraction structure of $\mathbf{1_2{\cdot}Bi_2{\cdot}(OTf)_6}$ in the solid state; (b) expansion of the structure, indicating the coordination at Bi; (c) minimized structure of $\mathbf{1_3{\cdot}Bi_2}$ (SPARTAN, AM1 force field); (d) minimized structure of $\mathbf{1_4{\cdot}Bi_2{\cdot}(OTf)_2}$ (SPARTAN, AM1 force field).

$\mathbf{1_4{\cdot}Bi_2}$) was observed as its +2 cation, with no triflate counterions observed. The charge state can be rationalized by loss of multiple TfOH molecules from the self assembly upon ionization, with the additional proton provided by the NH in the hydrazone group. This loss of the labile NH proton upon ionization is precedented for hydrazone-based self-assemblies.[18]

The most prevalent complex in the mass spectrum was the $\mathbf{1_2{\cdot}Bi_2}$ assembly, and the monocationic form was also observed, with retention of one TfO^- ion. Samples with varying concentrations of Bi were analyzed by ESI-MS, and in all cases, the three complexes were observed. Mass spectra were obtained from samples containing 0.5, 1, and 2 mol eq. $Bi(OTf)_3$ in an attempt to favor formation of the $\mathbf{1_3{\cdot}Bi_2}$ and $\mathbf{1_4{\cdot}Bi_2}$ complexes. Loss of ligand *via* fragmentation processes occurred in each, favoring the $\mathbf{1_2{\cdot}Bi_2}^{2+}$ ion, although an increase in the amount of $\mathbf{1_4{\cdot}Bi_2}$ was observed in the sample with small amounts (0.5 eq.) of $Bi(OTf)_3$.

The combination of MS and NMR data indicates that the binding energies of complexation are relatively weak: excess Bi was required to favor formation of the M_2L_2 complex. The equilibrium process was analyzed to determine the relative favorabilities. While the two equilibrium constants $\mathbf{K_1}$ (for the M_2L_4–M_2L_3 conversion) and $\mathbf{K_2}$ (for the M_2L_3–M_2L_2 conversion) are linked, the values can be calculated by analysis of the NMR spectra where only two species are observed (*i.e.* Fig. 2b and 2d), assuming (within error) that the concentration of any other species is zero. The initial equilibrium constant $\mathbf{K_1}$ is 162 M^{-1} at ambient temperature, showing that the $\mathbf{1_4{\cdot}Bi_2}$ complex is indeed disfavored. The second equilibrium constant $\mathbf{K_2}$ is 8 M^{-1}, indicating the similar stability of the $\mathbf{1_3{\cdot}Bi_2}$ and $\mathbf{1_2{\cdot}Bi_2}$ complexes. Due to the insolubility of **1** and its subsequent dissolution as $Bi(OTf)_3$ is added, an equilibrium constant for the initial formation of $\mathbf{1_4{\cdot}Bi_2}$ from **1** + $Bi(OTf)_3$ could not reasonably be established by NMR.

X-Ray quality crystals of this complex were obtained from diffusion of chloroform into a solution of preformed complex in acetonitrile. As the assembly process forms an equilibrium mixture of three products, solid state analysis was limited to that of complex $\mathbf{1_2{\cdot}Bi_2{\cdot}(OTf)_6}$, the most favorable assembly. While crystallizations were attempted with a range of bismuth concentrations, no other species were obtained. In the solid state, the $\mathbf{1_2{\cdot}Bi_2{\cdot}(OTf)_6}$ assembly forms as a quasi-coordination polymer, with two triflate counterions providing weak bridging interactions between each discrete M_2L_2 unit (Fig. 4a and 4b). This polymeric structure is more stable than the M_2L_3 or M_2L_4 structures, which display fewer Bi–O contacts. Each Bi ion provides nine coordination sites, three for each ligand and one for each of the three triflate counterions. Two triflates are bridged between each M_2L_2 complex and a third coordinates individually. There is also an additional triflate uncoordinated in the crystal structure, balancing the charge on the Bi(III) ions. The presence of three coordinating (but labile) triflate ions indicates the probability of coordinating three equivalents of ligand **1** around each Bi ion, forming the M_2L_3 system observed in both the ^1H NMR and ESI-MS spectra. The expected geometry of the complexes is shown by molecular minimization in Fig. 4c and 4d.

The structure of the M_2L_4 species is less obvious, however. Molecular minimizations suggest that self-assembly involving four ligands is possible if the coordination occurs *via* only two atoms, the imine nitrogen and the hydrazide oxygen, with the pyridine species uncoordinated as shown in Fig. 4d. Integration of the ^1H NMR spectrum shows that only one proton (imine H_2) is shifted downfield in the M_2L_4 assembly (as opposed to $\mathbf{1_2{\cdot}Bi_2}$ or $\mathbf{1_3{\cdot}Bi_2}$, where both H_1 and H_2 are shifted downfield more than 1 ppm). This coordination mode is not the most favored, as might be expected, but is suitably stable for observation at low concentrations of $Bi(OTf)_3$. Bidentate coordination *via* the two nitrogens of the pyridyl and imine groups is conceivable, but minimization of this possible structure was far less favorable due to geometrical constraints. A search of the Cambridge Crystallographic Database showed that four N–O bidentate ligands can form a BiL_4 coordination complex, providing precedent for the proposed structure.[19]

The assembly process is reversible: once the $\mathbf{1_2{\cdot}Bi_2{\cdot}(OTf)_6}$ complex is formed, addition of extra ligand **1** to the system drives the equilibrium backwards (Fig. 5). Upon addition of small amounts of ligand **1**, peaks for $\mathbf{1_3{\cdot}Bi_2}$ grew in to the spectrum, and a mixture of the $\mathbf{1_2{\cdot}Bi_2}$ and $\mathbf{1_3{\cdot}Bi_2}$ complexes was

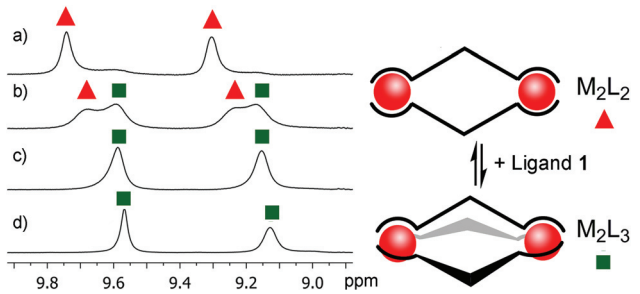

Fig. 5 ^{1}H NMR titration of ligand **1** into the preformed **1_2·Bi$_2$** complex: (a) **1_2·Bi$_2$**; (b) 1.0 eq.; (c) 1.8 eq.; (d) 2.9 eq.; (400 MHz, CD_3CN).

observed. A similar pattern to the forward titration emerged, and with increasing ligand concentration (decreased bismuth concentration), the **1_3·Bi$_2$** complex was solely observed. The insolubility of the ligand prevented formation of a completely pure M_2L_4 complex, but peaks were observed after addition of an excess of ligand (for full spectra, see ESI†).

The reversibility of the assembly in solution (and the presence of all three species in the ESI-MS) is somewhat at odds with the observation of a quasi-coordination polymer for **1_2·Bi$_2$·(OTf)$_6$** in the solid state. In solution, it is most likely that **1_2·Bi$_2$·(OTf)$_6$** exists as a discrete species whereby no bridging interactions occur between triflate ions. DOSY NMR (stimulated echo experiment, stebpgp1s pulse sequence, Fig. 6) was performed to determine the relative size and mobility of each complex. DOSY analysis of a mixture of the **1_3·Bi$_2$** and **1_4·Bi$_2$** complexes, gave observable, but small differences in diffusion coefficient. Complex **1_4·Bi$_2$** diffuses through CD_3CN slightly faster than **1_3·Bi$_2$** (D = 6.32 × 10^{-10} m^2 s^{-1} for **1_4·Bi$_2$**, D = 4.34 × 10^{-10} m^2 s^{-1} for **1_3·Bi$_2$**). As expected, M_2L_2 complex **1_2·Bi$_2$** displayed a similar diffusion coefficient to the other species in CD_3CN (D = 5.45 × 10^{-10} m^2 s^{-1} for **1_2·Bi$_2$**). These similar, albeit distinguishable, diffusion coefficients indicate that the three assemblies are of similar size and charge, and that the **1_2·Bi$_2$·(OTf)$_6$** is not a coordination polymer in solution. The values of the diffusion coefficients are similar to those of other metal–organic self-assemblies in CD_3CN, suggesting they exist as discrete complexes rather than extended coordination polymers.[20]

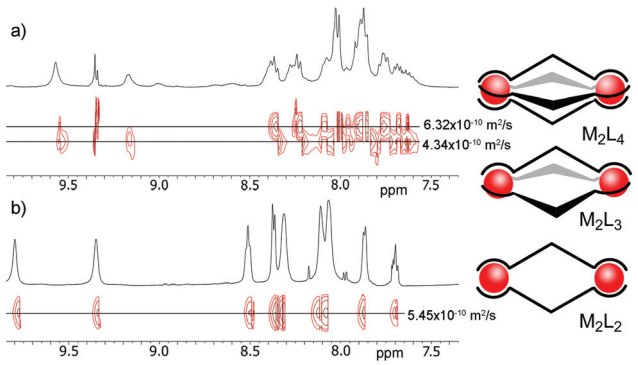

Fig. 6 (a) DOSY spectrum of **1** + 0.67 eq. $Bi(OTf)_3$ (CD_3CN, 600 MHz, 298 K, Δ = 17.0 ms, δ = 7000 μs, Diffusion coefficient = 6.32 × 10^{-10} m^2 s^{-1} for M_2L_4, 4.34 × 10^{-10} m^2 s^{-1} for M_2L_3, and 3.06 × 10^{-9} m^2 s^{-1} for CD_3CN); (b) DOSY spectrum of **1** + 3 eq. $Bi(OTf)_3$ (CD_3CN, 600 MHz, 298 K, Δ = 17.0 ms, δ = 7000 μs, diffusion coefficient = 5.45 × 10^{-10} m^2 s^{-1} and 3.80 × 10^{-9} m^2 s^{-1} for CD_3CN).

The assemblies were not soluble in $CDCl_3$ or D_2O, and complexation of Bi by the neutral ligand was not observed in competitive solvents such as DMSO-d_6. The deprotonated analog of ligand **1** (*i.e.* **1·Na$_2$**) is a stronger coordinator, however, and was accessible in quantitative yield upon treatment of **1** with base. Unlike ligand **1**, ligand **1·Na$_2$** was able to self-assemble with $Bi(OTf)_3$ in DMSO-d_6 as well as CD_3CN, but no appreciable change in composition of the self-assembled products was observed: all three distinct species were observed in the ^{1}H NMR spectrum upon titration with $Bi(OTf)_3$, and the M_2L_2 was favored at higher Bi concentrations, as with neutral **1** (see ESI†).

The presence of triflate ions in the crystal structure leads to the question of whether the self-assembly is mediated by the concentration of Bi(III) cations in the system alone, or whether the triflate counterions themselves are competitive ligands for the Bi ions. To study the assembly process in the absence of oxygen-containing counterions, $Bi(BF_4)_3$ was synthesized and applied to the ligand in CD_3CN. In this case, only one complex was observed, with a ^{1}H NMR spectrum almost identical to that of the M_2L_4 species observed in Fig. 2a and b (see ESI†). This M_2L_4 aggregate was disrupted by addition of excess NaOTf to the system, indicating that OTf^- ions are indeed good coordinators for Bi(III) and interrupt the formation of assemblies with greater ligand coordination. More strongly coordinating counterions were less effective. When $BiBr_3$ was added to the neutral ligand **1** in CD_3CN, no complexation occurred. The bromide ions are far more strongly coordinating than triflate ions, and cannot be displaced by the neutral ligand. Titration of $BiBr_3$ into a DMSO-d_6 solution of the more strongly coordinating anionic ligand **1·Na$_2$** (to more strongly favor coordination) showed complex coordination at low concentrations of Bi, but converged rapidly after addition of 1 mol eq. $BiBr_3$ to display a ^{1}H NMR spectrum almost identical to that of **1_2·Bi$_2$·(OTf)$_6$** (see ESI†). This system was not amenable to ESI-MS analysis, but evidently the Br^- ions are retained upon complexation with **1·Na$_2$** and cannot be displaced, leading to formation of M_2L_2 complexes only.

The V-shaped ligand **1** is restricted by geometry to formation of the M_2L_{2-4} coordination described above. To access larger polygonal assemblies, linear ligand **2** was used. Changing the ligand coordination angle removes the possibility of forming M_2L_x complexes of **2** for simple geometrical reasons: while linear ligand **2** contains the requisite coordination motif for Bi-mediated self-assembly, it is unable to provide suitable coordination angles to form the observed M_2L_x structures of **1**. Ligands with geometries such as this are precedented to form either M_nL_n polygons,[3] or larger self-assembled polyhedra.[7] Ligand **2**, similarly to ligand **1**, displayed insolubility in CD_3CN until exposed to added bismuth triflate, which caused dissolution. Ligand **2** was a much less effective coordinator for $Bi(OTf)_3$ than **1**, presumably due to the inability to form the favorable helix-type M_2L_3 assemblies above. Titration of

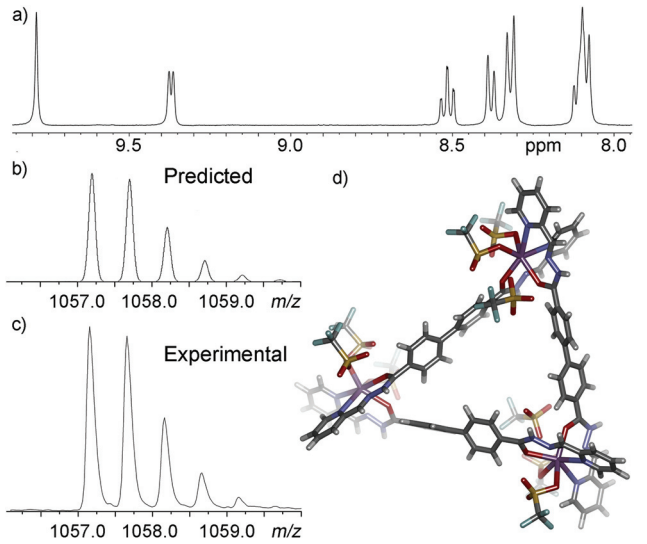

Fig. 7 Formation of an M_3L_3 triangle. (a) ^{1}H NMR spectrum (CD_3CN, 400 MHz, 298 K) of the complex $\mathbf{2_3{\cdot}Bi_3{\cdot}(OTf)_9}$; (b) predicted isotope pattern of $\mathbf{[2_3{\cdot}Bi_3{\cdot}(OTf)]^{2+}}$; (c) partial ESI-MS spectrum of M_3L_3 complex $\mathbf{2_3{\cdot}Bi_3{\cdot}(OTf)_9}$; (d) minimized structure of $\mathbf{2_3{\cdot}Bi_3{\cdot}(OTf)_9}$ (SPARTAN).

$Bi(OTf)_3$ into a CD_3CN suspension of **2** caused ligand dissolution, but no discrete self-assembled species were observed at low concentrations of Bi, rather a series of unidentified polymeric aggregates. A single species was formed only after addition of 2 equivalents of $Bi(OTf)_3$, and only one discrete species was formed in this case, rather than the reversible coordination motif displayed by **1** (see Fig. 7a; for full spectra, see ESI†). The complexation of Bi caused the expected downfield shifts in ligand peaks in the ^{1}H NMR spectrum, with the greatest shift observed in the imine peak H_2 and the *ortho*-pyridyl proton H_1 with peaks in the complex at δ 9.80 and 9.35 ppm respectively. ESI-MS analysis (see ESI†) of the $\mathbf{2_x{\cdot}Bi_x}$ complex was less conclusive than for ligand **1**, however. Many species were observed in the ESI spectrum, and were assigned as multiple fragments and MeCN adducts. The prevalent M^+ species was a $\mathbf{2_3{\cdot}Bi_3}$ assembly, with peaks observed for a +3 species observed at m/z = 655 (corresponding to deprotonation of ligand and loss of TfOH), and a +2 cation (with one TfO^- anion) of the same species present at m/z = 1057. Both peaks showed isotope patterns consistent with the presence of three Bi atoms.

Fig. 7b and 7c show the predicted and observed isotope pattern for $\mathbf{2_3{\cdot}Bi_3}$. While we were unsuccessful in obtaining a single crystal of suitable quality for X-ray diffraction analysis, molecular modeling suggests a self-assembled M_3L_3 triangle with similar coordination geometry at Bi as for the crystal structure obtained for $\mathbf{1_2{\cdot}Bi_2{\cdot}(OTf)_6}$, with three triflate counterions occupying sites at the metal (Fig. 7d). While a quasi-polymeric structure might be expected in the solid state for $\mathbf{2_3{\cdot}Bi_3{\cdot}(OTf)_9}$, such a structure would contain large holes, possibly disfavoring crystallization. DOSY NMR analysis of the $\mathbf{2_3{\cdot}Bi_3{\cdot}(OTf)_9}$ species showed that the measured diffusion coefficient (D = 4.88 × 10^{-10} m^2 s^{-1}) was similar to that observed for the previously analyzed $\mathbf{1_{2-4}{\cdot}Bi_2}$ species in solution. This indicates that the charge and size properties of $\mathbf{2_3{\cdot}Bi_3{\cdot}(OTf)_9}$ are similar to those of $\mathbf{1_2{\cdot}Bi_2{\cdot}(OTf)_6}$. Experiments to favor increased coordination at the metal and formation of larger constructs (*e.g.* use of $Bi(BF_4)_3$) were unsuccessful: the linear coordination geometry is less favorable for Bi complexation than **1**, and only the M_3L_3 triangle is observed.

Conclusion

In conclusion, we have shown that Bi(III) ions can be used for mild, *reversible* self-assembly of suitable coordinating ligands, while exploiting the maximum number of binding sites at the metal. By varying the coordination angle of the ligands, different self-assembled polygons can be accessed: V-shaped ligands lead to either M_2L_2, M_2L_3 or M_2L_4 complexes, with the proportions controlled by bismuth concentration. The complexes are air and water stable, and soluble in common organic solvents.

The formation of these complexes is rapid and reversible, with addition of either ligand or Bi salts forcing the equilibrium to reactants or products, respectively. In contrast, linear coordinating ligands show formation of a mixture of unidentified oligomeric aggregates until, upon treatment with excess Bi(III), formation of a single M_3L_3 triangle is favored. Further study of reversible Bi-mediated supramolecular assembly and its application in the formation of larger polyhedral structures and switchable self-assemblies is currently underway in our laboratory.

Experimental

General information

^{1}H and ^{13}C spectra were recorded on a Varian Inova 400 or Varian Inova 500 spectrometer. Proton (^{1}H) chemical shifts are reported in parts per million (δ) with respect to tetramethylsilane (TMS, δ = 0), and referenced internally with respect to the protio solvent impurity. Deuterated NMR solvents were obtained from Cambridge Isotope Laboratories, Inc., Andover, MA, and used without further purification. Mass spectra were recorded on an Agilent 6210 LC TOF mass spectrometer using electrospray ionization and processed with an Agilent MassHunter Operating System. X-ray intensity data were collected at 100(2) K on a Bruker APEX2 platform-CCD X-ray diffractometer system. All other materials were obtained from Aldrich Chemical Company, St. Louis, MO or Combi-Blocks, San Diego, CA and were used as received. Solvents were dried through a commercial solvent purification system (Pure Process Technologies, Inc.). Molecular modeling (semi-empirical calculations) was performed using the AM1 force field using SPARTAN.[21]

Experimental procedures

Synthesis of compounds

1,1′:3′,1″-Terphenyl-4,4″-dicarbohydrazide (3). To a round bottom flask equipped with stir bar and reflux condenser was

added 1,3-dibromobenzene (600 mg, 2.54 mmol), 4-ethoxycarbonylphenylboronic acid (1.23 g, 6.35 mmol), bis(triphenylphosphine)palladium(II) chloride (90 mg, 0.13 mmol), and cesium carbonate (2.49 g, 7.65 mmol). The mixture was placed under nitrogen and anhydrous *N*,*N*-dimethylformamide (10 mL) was added. The reaction was heated under nitrogen at 100 °C for 16 h. Methanol (20 mL) was added and the reaction was filtered. The filtrate was allowed to cool in an ice bath, and the resultant precipitate was filtered. The crude product was dissolved in methylene chloride (5 mL) and filtered through a celite plug topped with a thin layer of silica gel. The filtrate was evaporated under reduced pressure to yield diethyl 1,1′:3′,1″-terphenyl-4,4″-dicarboxylate as a white solid (610 mg, 64%). ^{1}H NMR (400 MHz, $CDCl_3$) δ 8.14 (d, J = 8.4 Hz, 4H); 7.85 (t, J = 2.0 Hz, 1H); 7.71 (d, J = 8.4 Hz, 4H); 7.65 (dd, J = 1.6, 6.8 Hz, 2H); 7.57 (dd, J = 6.8, 8.4 Hz, 1H); 4.42 (q, J = 7.1 Hz, 4H); 1.43 (t, J = 7.1 Hz, 6H); ^{13}C NMR (100 MHz, $CDCl_3$) δ 166.6; 145.3; 141.0; 130.3; 129.70; 129.65; 127.3; 127.2; 126.4; 61.2; 14.5; HRMS (ESI) m/z calcd for $C_{24}H_{23}O_4$ $(M + H)^+$ 375.1591; found 375.1601.

This ester (254 mg, 0.68 mmol) and hydrazine (3 mL) were then added to a round bottom flask equipped with stir bar and reflux condenser. The reaction was stirred at 85 °C for 18 h before water (5 mL) was added and the precipitate filtered to yield **3** as a white solid (203 mg, 86%). ^{1}H NMR (400 MHz, DMSO-d_6) δ 9.86 (s, 2H); 8.02 (s, 1H); 7.76 (d, J = 8.2 Hz, 4H); 7.88 (d, J = 8.3 Hz, 4H); 7.75 (d, J = 7.7 Hz, 2H); 7.60 (t, J = 7.8 Hz, 1H); 4.54 (br s, 4H); ^{13}C NMR (100 MHz, DMSO-d_6) δ 165.6; 142.5; 140.0; 132.3; 129.8; 127.6; 126.9; 126.6; 125.5; HRMS (ESI) m/z calcd for $C_{20}H_{19}N_4O_2$ $(M + H)^+$ 347.1503; found 347.1536.

*1,1′:3′,1″-Terphenyl-4,4″-dicarboxylic acid, bis-(2-pyridinylmethylene)-hydrazide (**1**).* To a round bottom flask equipped with stir bar and reflux condenser was added hydrazide **3** (176 mg, 0.51 mmol), 2-pyridinecarboxaldehyde (112 μL, 1.27 mmol), ethanol (5 mL), and acetic acid (2 drops). The reaction was refluxed for 16 h, cooled in an ice bath, and washed with cold ethanol to yield **1** as a white solid (208 mg, 78%). ^{1}H NMR (400 MHz, DMSO-d_6) δ 12.17 (s, 2H); 8.62 (d, J = 4.8 Hz, 2H); 8.52 (s, 2H); 8.08 (m, 5H); 8.03 (d, J = 8.0 Hz, 2H); 7.98 (d, J = 7.7 Hz, 4H); 7.90 (t, J = 7.6 Hz, 2H); 7.81 (d, J = 7.6 Hz, 2H); 7.64 (t, J = 7.8 Hz, 1H); 7.43 (t, J = 6.3 Hz, 2H); ^{13}C NMR (100 MHz, DMSO-d_6) δ 163.3; 153.4; 149.7; 148.2; 143.5; 140.1; 137.1; 132.2; 130.0; 128.6; 127.2; 127.0; 125.7; 124.6; 120.2; HRMS (ESI) m/z calcd for $C_{32}H_{25}N_6O_2$ $(M + H)^+$ 525.2034; found 525.1983.

*1,1′-Biphenyl-4,4′-dicarbohydrazide (**4**).* To a round bottom flask equipped with stir bar was added 4,4′-biphenyl dicarboxylic acid (1.00 g, 4.13 mmol), 2-(6-chloro-1*H*-benzotriazole-1-yl)-1,1,3,3-tetramethylaminium hexafluoro-phosphate [HCTU] (3.44 g, 8.32 mmol), acetonitrile (40 mL), and triethylamine (2.5 mL, 17.8 mmol). The reaction was stirred at room temperature for 5 h, followed by addition of triethylamine (2.5 mL, 17.8 mmol) and anhydrous hydrazine (300 μL, 9.60 mmol). The reaction was stirred at room temperature for an additional 16 h, followed by filtering a white precipitate, which was then rinsed with deionized water (200 mL), triturated in dichloromethane (50 mL), and refiltered to give **4** as an off-white solid (848 mg, 76%). ^{1}H NMR (400 MHz, DMSO-d_6) δ 9.91 (br, 2H); 7.94 (d, J = 8.4 Hz, 4H); 7.84 (d, J = 8.4 Hz, 4H); 4.83 (br, 4H); ^{13}C NMR (100 MHz, DMSO-d_6) δ 165.4; 141.6; 132.5; 127.7; 126.7; HRMS (ESI) m/z calcd for $C_{14}H_{14}N_4O_2$ $(M + H)^+$ 271.1189; found 271.1204.

*1,1′-Biphenyl-4,4′-dicarboxylic acid, bis-(2-pyridinylmethylene)-hydrazide (**2**).* To a round bottom flask equipped with stir bar and reflux condenser was added hydrazide **4** (500 mg, 5.27 mmol), 2-pyridinecarboxaldehyde (500 μL, 5.27 mmol), absolute ethanol (15 mL), and acetic acid (2 drops). The reaction was refluxed 24 h under N_2. After cooling to room temperature, a white precipitate was filtered and washed with 95% ethanol (100 mL) to give product **2** as a white solid (857 mg, 91%). ^{1}H NMR (400 MHz, DMSO-d_6) δ 12.15 (s, 2H); 8.62 (d, J = 4.3 Hz, 2H); 8.54 (s, 2H); 8.08 (d, J = 8.1 Hz, 4H); 8.00 (d, J = 7.6 Hz, 2H); 7.94 (d, J = 8.1 Hz, 4H); 7.88 (t, J = 7.4 Hz, 2H); 7.42 (t, J = 5.4 Hz, 2H); ^{13}C NMR (100 MHz, DMSO-d_6) δ 162.9; 153.3; 149.5; 148.2; 142.3; 136.9; 132.6; 128.5; 127.0; 124.4; 119.9; HRMS (ESI) m/z calcd for $C_{26}H_{20}N_6O_2$ $(M + H)^+$ 449.1721; found 449.1708.

Synthesis and characterization of self-assembled complexes

1_2Bi_2·(OTf)$_6$ complex. Ligand **1** (5.0 mg, 0.01 mmol) and Bi(OTf)$_3$ (18.8 mg, 0.03 mmol) were combined in an NMR tube with 0.5 mL CD_3CN. The mixture was shaken for 10 s for quantitative formation of **1_2Bi_2·(OTf)$_6$**. ^{1}H NMR (400 MHz, CD_3CN) δ 9.77 (s, 2H); 9.34 (s, 2H); 8.49 (t, J = 7.8 Hz, 2H); 8.35 (d, J = 7.6 Hz, 2H); 8.31 (d, J = 8.0 Hz, 4H); 8.14 (s, 1H); 8.08 (m, 6H); 7.87 (d, J = 8.0 Hz, 2H); 7.70 (t, J = 7.8 Hz, 1H); ^{13}C NMR (100 MHz, CD_3CN) δ 169.0; 154.1; 153.0; 148.4; 144.1; 140.7; 131.4; 131.1; 131.0; 129.2; 128.9; 127.5; 126.7; 122.8; 119.6. HRMS (ESI) m/z calcd for $C_{78}H_{54}Bi_3N_{18}O_6$ (M-4(TfOH)-2(OTf))$^{2+}$ 731.1602; found 655.1290.

2_3Bi_3·(OTf)$_9$ complex. Ligand **2** (10.0 mg, 0.02 mmol) and Bi(OTf)$_3$ (29.3 mg, 0.04 mmol) were combined in an NMR tube with 0.5 mL CD_3CN. The mixture was shaken for 10 s for quantitative formation of **2_3Bi_3·(OTf)$_9$**. ^{1}H NMR (400 MHz, CD_3CN) δ 9.79 (s, 2H), 9.37 (d, J = 5.1 Hz, 2H); 8.51 (t, J = 7.7 Hz, 2H); 8.38 (d, J = 7.6 Hz, 2H); 8.31 (d, J = 8.4 Hz, 4H); 8.11 (partially overlapped t, J = 6.6 Hz, 2H); 8.08 (d, J = 8.4 Hz, 4H); 5.58 (br, 2H); (100 MHz, CD_3CN) δ 168.9; 154.4; 153.0; 148.4; 146.7; 144.2; 131.1; 129.6; 127.9; 125.9; 121.1 (q, J = 318.6 Hz); HRMS (ESI) m/z calcd for $C_{78}H_{54}Bi_3N_{18}O_6$ (M-6(TfOH)-3(OTf))$^{3+}$ 655.1289; found 655.1290.

NMR titration procedure. Ligand **1** (4.4 mg, 0.008 mmol) and 0.5 mL CD_3CN were combined in an NMR tube, and a solution of Bi(OTf)$_3$ was added at 0.25, 0.33, 0.50, 0.67, 0.75 1, 1.5, and 2 eq. with shaking to mix at each addition.

X-ray structure determination

Crystal data. Crystals of **1_2·Bi$_2$·(OTf)$_6$** suitable for X-ray diffraction analysis were obtained by slow diffusion of chloroform into a solution of complex in acetonitrile. A colorless fragment of a prism (0.35 × 0.17 × 0.07 mm^3) was used for the single crystal X-ray diffraction study of $[C_{32}H_{24}N_6O_2]_2[Bi]_2[SO_3CF_3]_6$

(CCDC submission #892045). The crystal was coated with paratone oil and mounted on to a cryo-loop glass fiber. X-ray intensity data were collected at 100(2) K on a Bruker APEX2 platform-CCD X-ray diffractometer system (fine focus Mo-radiation, λ = 0.71073 Å, 50 kV/35 mA power). The CCD detector was placed at a distance of 5.0000 cm from the crystal. $[C_{32}H_{24}N_6O_2]_2[Bi]_2[SO_3CF_3]_6$[partial solvents], M = 1391.94 [including partially occupied solvents], triclinic space group $P\bar{1}$ (no. 2), a = 10.5697(3) Å, b = 13.7043(4) Å, c = 20.0249(6) Å, α = 98.057(1), β = 92.112(1)°, γ = 96.452(1), V = 2849.71(14) Å^3, Z = 2, calculated density D_c = 1.622 g cm^{-3}, V = 2849.71(14) Å^3, Z = 2, calculated density D_c = 1.622 g cm^{-3}, colorless prism fragment (0.35 × 0.17 × 0.07 mm^3) coated with paratone oil, T = 100(2) K, 68 323 reflections measured (0.77 Å resolution), 13 040 unique (R_{int} = 0.0256, completeness = 99.8%), final R_1 = 0.0293, wR_2 = 0.0774 with intensity $I > 2\sigma(I)$ (see ESI† for full experimental).

Procedure for diffusion experiments

Diffusion experiments were performed using a Bruker Avance 600 MHz NMR spectrometer equipped with a broadband inverse probe with *x*-, *y*-, and *z*-gradients. Chemical shifts were referenced to the acetonitrile-d(2) resonance (1.94) ppm. Diffusion datasets were acquired using the stimulated echo experiment with bipolar gradients (stebpgp1s) included with the Topspin release version 1.3. Gradient amplitudes were incremented as a square dependence from 5% to 95% into 64 or 96 gradient increments. A spoil gradient pulse of length 1 ms and amplitude of −17.13% was used to effectively remove transverse magnetization following the encode period of the pulse program. Spectra were acquired with 128 transients coadded and 28 672 data points per transient for each of the 64 or 96 increments. Diffusion (Δ) and gradient pulse times (δ) were optimized using a one-dimensional version of the stimulated echo pulse sequence, stebpgp1s1d to give values of 17 and 7 ms, respectively. Diffusion coefficients were calculated using the processing features in Topspin by Bruker.

Calculation of equilibrium constants

1_4·Bi$_2$ and 1_3·Bi$_2$. Only complexes **1_4·Bi$_2$** and **1_3·Bi$_2$** were observed at equilibrium so contributions from **1** and **1_2·Bi$_2$** were assumed to be negligible. Concentrations of each complex from a mixture of 9.91 × 10^{-3} mmol **1**, 7.42 × 10^{-3} mmol Bi(OTf)$_3$, and 0.545 mL DMSO were determined by integrating the ^{1}H NMR from 9.60–9.48 ppm and 9.38–9.31 ppm.

$$[\mathbf{1_4 \cdot Bi_2}] = 2.72 \times 10^{-3}\ \text{M};\ [\mathbf{1_3 \cdot Bi_2}] = 2.44 \times 10^{-3}\ \text{M};\ [\mathbf{Bi}] = 3.30 \times 10^{-3}\ \text{M}$$

$$3\ M_2L_4 + 2\ M \rightarrow 4\ M_2L_3$$

$$K_1 = \frac{[M_2L_3]^4}{[M_2L_4]^3[M]^2} = 162 \pm 16\ \text{M}^{-1}$$

1_3·Bi$_2$ and 1_2·Bi$_2$. Only complexes **1_3·Bi$_2$** and **1_2·Bi$_2$** were observed at equilibrium so contributions from **1** and **1_4·Bi$_2$** were assumed to be negligible. Concentrations of each complex from a mixture of 9.91 × 10^{-3} mmol **1**, 1.98 × 10^{-2} mmol Bi(OTf)$_3$, and 0.620 mL DMSO were determined by integrating the ^{1}H NMR from 9.78–9.65 ppm and 9.65–9.51 ppm.

$$[\mathbf{1_3 \cdot Bi_2}] = 3.27 \times 10^{-3}\ \text{M};\ [\mathbf{1_2 \cdot Bi_2}] = 3.1 \times 10^{-3}\ \text{M};\ [\mathbf{Bi}] = 1.92 \times 10^{-2}\ \text{M}$$

$$2\ M_2L_3 + 2\ M \rightarrow 3\ M_2L_2$$

$$K_2 = \frac{[M_2L_2]^3}{[M_2L_3]^2[M]^2} = 8 \pm 1\ \text{M}^{-1}$$

Acknowledgements

The authors would like to thank Dr Fook Tham for X-ray crystallographic analysis, Ron New for mass spectral analysis, Dr Dan Borchardt for assistance with DOSY-NMR, and the National Science Foundation (CHE-1151773) for support of this research.

Notes and references

1 (*a*) M. M. J. Smulders, A. Jiménez and J. R. Nitschke, *Angew. Chem., Int. Ed.*, 2012, **51**, 6681; (*b*) Y.-R. Zheng, Z. Zhao, M. Wang, K. Ghosh, J. B. Pollock, T. R. Cook and P. J. Stang, *J. Am. Chem. Soc.*, 2010, **132**, 16873; (*c*) T. Murase, Y. Nishijima and M. Fujita, *J. Am. Chem. Soc.*, 2012, **134**, 162; (*d*) R. W. Saalfrank, H. Maid, A. Scheurer, F. W. Heinemann, R. Puchta, W. Bauer, D. Stern and D. Stalke, *Angew. Chem., Int. Ed.*, 2008, **47**, 8941; (*e*) M. Eddaoudi, J. Kim, N. Rosi, D. Vodak, J. Wachter, M. O'Keeffe and O. M. Yaghi, *Science*, 2002, **295**, 469; (*f*) J. J. Lessmann and J. W. D. Horrocks, *Inorg. Chem.*, 2000, **39**, 3114; (*g*) R. Chakrabarty, P. S. Mukherjee and P. J. Stang, *Chem. Rev.*, 2011, **111**, 6810; (*h*) M. Albrect, *Chem. Rev.*, 2001, **101**, 3456; (*i*) P. T. Corbett, J. Leclaire, L. Vial, K. R. West, J.-L. Wietor, J. K. M. Sanders and S. Otto, *Chem. Rev.*, 2006, **106**, 3652.

2 (*a*) B. J. Holliday and C. A. Mirkin, *Angew. Chem., Int. Ed.*, 2001, **40**, 2022; (*b*) K. Harano, S. Hiraoka and M. Shionoya, *J. Am. Chem. Soc.*, 2007, **129**, 5300; (*c*) S. Hiraoka, T. Yi, M. Shiro and M. Shionoya, *J. Am. Chem. Soc.*, 2002, **124**, 14510.

3 (*a*) R. Kieltyka, P. Englebienne, J. Fakhoury, C. Autexier, N. Moitessier and H. F. Sleiman, *J. Am. Chem. Soc.*, 2008, **130**, 10040; (*b*) M. Schmittel and K. Mahata, *Chem. Commun.*, 2010, **46**, 4163; (*c*) S. Shanmugaraju, V. Vajpayee, S. Lee, K.-W. Chi, P. J. Stang and P. S. Mukherjee, *Inorg. Chem.*, 2012, **51**, 4817; (*d*) H. Abourahma, B. Moulton, V. Kravtsov and M. J. Zaworotko, *J. Am. Chem. Soc.*, 2002, **124**, 9990; (*e*) K. J. Kilpin, M. L. Gower, S. G. Telfer, G. B. Jameson and J. D. Crowley, *Inorg. Chem.*, 2011, **50**, 1123; (*f*) J. R. Nitschke, M. Hutin and G. Bernardinelli, *Angew. Chem., Int. Ed.*, 2004, **43**, 6724; (*g*) G. S. Papaefstathiou,

T. D. Hamilton, T. Friščić and L. R. MacGillivray, *Chem. Commun.*, 2004, 270–271.

4 (*a*) A. M. Johnson, O. Moshe, A. S. Gamboa, B. W. Langloss, J. F. K. Limtiaco, C. K. Larive and R. J. Hooley, *Inorg. Chem.*, 2011, **50**, 9430; (*b*) M. D. Pluth, D. Fiedler, J. S. Mugridge, R. G. Bergman and K. N. Raymond, *Proc. Natl. Acad. Sci. U. S. A.*, 2009, **106**, 10438; (*c*) D. Fujita, A. Takahashi, S. Sato and M. Fujita, *J. Am. Chem. Soc.*, 2011, **133**, 13317; (*d*) T. K. Ronson, J. Fisher, L. P. Harding, P. J. Rizkallah, J. E. Warren and M. J. Hardie, *Nat. Chem.*, 2009, **1**, 212; (*e*) W. Meng, B. Breiner, K. Rissanen, J. D. Thoburn, J. K. Clegg and J. R. Nitschke, *Angew. Chem., Int. Ed.*, 2011, **50**, 3479; (*f*) S. Sato, J. Iida, K. Suzuki, M. Kawano, T. Ozeki and M. Fujita, *Science*, 2006, **313**, 1273.

5 (*a*) P. Mal, B. Breiner, K. Rissanen and J. R. Nitschke, *Science*, 2009, **324**, 1697; (*b*) S. Turega, M. Whitehead, B. R. Hall, M. F. Haddow, C. A. Hunter and M. D. Ward, *Chem. Commun.*, 2012, **48**, 2752; (*c*) P. Liao, B. W. Langloss, A. M. Johnson, E. R. Knudsen, F. S. Tham, R. R. Julian and R. J. Hooley, *Chem. Commun.*, 2010, **46**, 4932; (*d*) J. K. Clegg, J. Cremers, A. J. Hogben, B. Breiner, M. M. J. Smulders, J. D. Thoburn and J. R. Nitschke, *Chem. Sci.*, 2013, **4**, 68.

6 (*a*) D. H. Leung, R. G. Bergman and K. N. Raymond, *J. Am. Chem. Soc.*, 2007, **129**, 2746; (*b*) M. Yoshizawa, M. Tamura and M. Fujita, *Science*, 2006, **312**, 251.

7 W. Meng, J. K. Clegg, J. D. Thoburn and J. R. Nitschke, *J. Am. Chem. Soc.*, 2011, **133**, 13652.

8 (*a*) D. L. Caulder and K. N. Raymond, *Acc. Chem. Res.*, 1999, **32**, 975; (*b*) M. Wang, V. Vajpayee, S. Shanmugaraju, Y.-R. Zheng, Z. Zhao, H. Kim, P. S. Mukherjee, K.-W. Chi and P. J. Stang, *Inorg. Chem.*, 2011, **50**, 1506.

9 (*a*) W. J. Vickaryous, E. R. Healy, O. B. Berryman and D. W. Johnson, *Inorg. Chem.*, 2005, **44**, 9247; (*b*) V. M. Cangelosi, L. N. Zakharov, S. A. Fontenot, M. A. Pitt and D. W. Johnson, *Dalton Trans.*, 2008, 3447; (*c*) V. M. Cangelosi, L. N. Zakharov and D. W. Johnson, *Angew. Chem., Int. Ed.*, 2010, **49**, 1248; (*d*) J. Zukerman-Schpector, A. Otero-de-la-Roza, V. Luaña and E. R. T. Tiekink, *Chem. Commun.*, 2011, **47**, 7608; (*e*) J. S. Mugridge, D. Fiedler and K. N. Raymond, *J. Coord. Chem.*, 2010, **63**, 2779; (*f*) R. García-Zarracino and H. Höpfl, *J. Am. Chem. Soc.*, 2005, **127**, 3120; (*g*) W. J. Vickaryous, R. Herges and D. W. Johnson, *Angew. Chem., Int. Ed.*, 2004, **43**, 5831; (*h*) S. T. Onions, A. M. Frankin, P. N. Horton, M. B. Hursthouse and C. J. Matthews, *Chem. Commun.*, 2003, 2864; (*i*) B. Najjari, S. Le Gac, T. Roisnel, V. Dorcet and B. Boitrel, *J. Am. Chem. Soc.*, 2012, **134**, 16017; (*j*) S. A. Fontenot, V. M. Cangelosi, M. A. W. Pitt, A. C. Sather, L. N. Zakharov, O. B. Berryman and D. W. Johnson, *Dalton Trans.*, 2011, **40**, 12125; (*k*) M. Pitt and D. W. Johnson, *Chem. Soc. Rev.*, 2007, **36**, 1441.

10 (*a*) P. C. Andrews, G. B. Deacon, C. M. Forsyth, P. C. Junk, I. Kumar and M. Maguire, *Angew. Chem., Int. Ed.*, 2006, **45**, 5638; (*b*) M. Rowinska-Zyrek, D. Valensin, L. Szyrwiel, Z. Grzonka and H. Kozlowski, *Dalton Trans.*, 2009, 9131; (*c*) N. Yang and H. Sun, *Coord. Chem. Rev.*, 2007, **251**, 2354; (*d*) N. Yang, J. A. Tanner, B.-J. Zheng, R. M. Watt, M.-L. He, L.-Y. Lu, J.-Q. Jiang, K.-T. Shum, Y.-P. Lin, K.-L. Wong, M. C. M. Lin, H.-F. Kung, H. Sun and J.-D. Huang, *Angew. Chem., Int. Ed.*, 2007, **46**, 6464.

11 (*a*) S. P. Summers, K. A. Abboud, S. R. Farrah and G. J. Palenik, *Inorg. Chem.*, 1994, **33**, 88; (*b*) D. T. Tran, D. Chu, A. G. Oliver and S. R. J. Oliver, *Inorg. Chem. Commun.*, 2009, **12**, 1081; (*c*) D. Mendoza-Espinosa, A. L. Rheingold and T. A. Hanna, *Dalton Trans.*, 2009, 5226; (*d*) A. A. Schilt and R. C. Taylor, *J. Inorg. Nucl. Chem.*, 1959, **9**, 211; (*e*) N. Tan, S. Yin, Y. Li, R. Qiu, Z. Meng, X. Song, S. Luo, C.-T. Au and W.-Y. Wong, *J. Organomet. Chem.*, 2011, **696**, 1579; (*f*) S. Roggan, C. Limberg, B. Ziemer and M. Brandt, *Angew. Chem., Int. Ed.*, 2004, **43**, 2846.

12 C. A. Stewart, J. C. Calabrese and A. J. Arduengo III, *J. Am. Chem. Soc.*, 1985, **107**, 3397.

13 J.-C. G. Bünzli and C. Piguet, *Chem. Rev.*, 2002, **102**, 1897.

14 V. M. Cangelosi, L. N. Zakharov and D. W. Johnson, *Angew. Chem., Int. Ed.*, 2010, **49**, 1248.

15 (*a*) X. Wu, Z. Lin, C. He and C. Duan, *New J. Chem.*, 2012, **36**, 161; (*b*) X. Zhu, C. He, D. Dong, Y. Liu and C. Duan, *Dalton Trans.*, 2010, **39**, 10051; (*c*) B. Wang, Z. Zang, H. Wang, W. Dou, X. Tang, W. Liu, Y. Shao, J. Ma, Y. Li and J. Zhou, *Angew. Chem., Int. Ed.*, 2013, **52**, 3756.

16 L. Yang, X. Wu, C. He, Y. Jiao and C. Duan, *Chem. Commun.*, 2009, 7554.

17 (*a*) J. Wang, H. Wu, C. He, L. Zhao and C. Duan, *Chem.–Asian J.*, 2011, **6**, 1225; (*b*) H. Wu, C. He, Z. Lin, Y. Liu and C. Duan, *Inorg. Chem.*, 2009, **48**, 408.

18 J. Wang, C. He, P. Wu, J. Wang and C. Duan, *J. Am. Chem. Soc.*, 2011, **133**, 12402.

19 O. Anjaneyulu, D. Maddileti and K. C. Kumara Swamy, *Dalton Trans.*, 2012, **41**, 1004.

20 (*a*) J. Bunzen, J. Iwasa, P. Bonakdarzadeh, E. Numata, K. Rissanen, S. Sato and M. Fujita, *Angew. Chem., Int. Ed.*, 2011, **51**, 3161; (*b*) W. Li, H. Chung, C. Daeffler, J. A. Johnson and R. H. Grubbs, *Macromolecules*, 2012, **45**, 9595.

21 M. J. S. Dewar, E. G. Zoebisch, E. F. Healy and J. J. P. Stewart, *J. Am. Chem. Soc.*, 1985, **107**, 3902; calculations performed on SPARTAN 06, Wavefunction Inc.